Performance Analysis of Notch Filtering Concept Based Reconfigurable Bow-Tie Shaped Patch Antenna for Wireless Application

Anwar Shahzad Siddiqui[1], Devesh Kumar*[2], M. R. Tripathy[3] and H. P. Singh[4]
[1,2] *Department of Electrical Engineering, JMI, New Delhi India,*
[3,4] *Amity University, Noida, Uttar Pradesh India,*

Abstract—*This paper comprises the designing of a antenna which is capable to reconfigure the operational frequency as well as mode of polarization. The designed MPA consists a bow-tie shaped patch, switchable ground and feed network. The feed network is made up with a Wilkinson's power divider, two 90^0 phase shifters and two spur-line filers. The phase shifters are competent to switch the mode of polarization between LHCP & RHCP where as spur-line filters are adept to reconfigure the operational frequencies. The feed network is controlled by utilizing PIN diodes. The designed MPA is competent to function either in monopole mode and DGS mode. The whole design is simulated with HFSS simulation tool. The results are adequate and fulfill the expectation.*

Keywords: **Frequency reconfiguration, polarization diversity, bow-tie microstrip patch, monopole and DGS**

1. INTRODUCTION

The use of electromagnetic spectrum for the open-link communication system is getting more and more clogged up day by day. So, the demand of increasing the use of EM spectrum needs a way to utilize the EM spectrum in switchable manner. Thus, the transmitting and receiving system must have switchable ability among various frequency bands and other performance characteristics of system like polarization, impedance, bandwidth, field pattern. So, the switchable ability of the antenna can be achieved by altering the distribution of current on the radiator. Redistribution of current is the cause of changes in EM wave scenario within the radiating patch and ground plane. Redistribution of electric current on the radiating patch can be done by using solid state switches like PIN diode, varactor diode, RFMEMS [7] etc. or by mechanically, or by other means such as tuneability of materials. The needs of reconfigurable antennas are widespread in upgraded generation in wireless communication and sensing systems [1].

A reconfigurable monopole antenna for the Global Navigation Satellite System is designed in [2] which consist of orthogonally oriented two meandered monopoles. A frequency reconfigurable bow-tie shaped radiator is presented in [3] which is proficient to tune over frequency range 3-6 GHz. A printed antenna is elaborated with designed concept and fabrication in [4] for multi-standard wireless application which is proficient to be reconfiguring in terms of frequency and pattern. Compact truncated monopole antenna is demonstrated with design technique and fabrication in [5] which is proficient to be in terms of radiation pattern (omni-directional) and polarization.

Particle swarm optimization based an electronically reconfigurable annular ring monopole antenna is well demonstrated in [6]. A Reconfigurable Microstrip Patch Antenna with Frequency and Circular Polarization Diversities (LHCP & RHCP) is detailed in [8], which consists of two parts: a patch with two orthogonal slots on the upper substrate and a 3dB hybrid-coupler fed structure which fabricated on the lower substrate. Various techniques and methodologies which are widely embraced for reconfigurable antennas are reviewed in [9]. Center-Shorted microstrip antenna is elaborated with design concept and operational principle in [10], which is proficient to be reconfiguring in terms of operational frequency and radiation pattern. Monopole Concept Based PA for mm-Wave 5G-Band Application is detailed in [11] which is able to be reconfiguring in terms of operational frequency. In [12], an ultra-wide band planar antenna is designed and printed which adopt band notch concept to filter out undesired frequency bands. In [13 & 14], spur-line band stop filtering concept is detailed.

2. ANTENNA DESIGN

The designed MPA comprises the bow-tie shaped patch and switchable bow-tie shaped ground plane as shown in fig. 2. The designed MPA is able to work for two modes of operations: DGS Mode and monopole mode. A dielectric substrate FR4-epoxy of dielectric constant of 4.4 is used for the simulation. The substrate's height of 1.0 mm is taken. PIN diodes are used as switching element. The ground plane is spread beneath the partial area of the patch as shown in fig. 4(a). Two switches S12 and S13 are employed in the ground plane to switch the operation of the MPA between DGS mode and monopole mode. When both the switches are ON, antenna works in DGS mode and if both the switches are kept on OFF state then it works in monopole mode. The metamaterial-inspired structure as shown in fig. 4(b) is inserted in the ground to enhance the antenna performance.

The shaped of the patch is bow-tie with curved shape at their open ends. The Both flare of bow-tie patch is fed separately using a feed system as shown in fig. 2 .The feed system comprises three sections as shown in fig. 3(a): The first section is filter part and it is used to switch the antenna operation between 3-4 GHz frequency band and 5-6 GHz frequency band. The second section which follows the first section is Wilkinson's power divider. The last section is 90^0 phase shifters (PS) and used to feed signals to radiating patches with various phase differences. The purpose of feeding signals with 90^0 phase difference is to reconfigure the polarization characteristic of the designed MPA.

A Wilkinson's power divider as depicted in fig. 1 (a) is three-port network that divides the power fed to its input port into two parts depending upon the design considerations. It's all three port are matched, and this matching is attained by deploying a resistive element in the three-port network [15]. A Wilkinson's power divider has better isolation as compared to a simple T-junction power divider.

The input port has Z0 = 50 Ω impedance. Thus, the impedance of other two ports (output) is set at 50 Ω so that division of power fed to its input port is made equally. In consideration of this, two λg /4 MTL transformers of 1.44*Z0 impedance are used as two arms of Wilkinson's power divider. Here λg is guided wavelength in the dielectric medium at operating frequency f0. Finally, a λg /4 MS-Line transformer of impedance [Sqrt (50*Input-impedance of the patch] is used in between 50 Ω line and radiating patch to feed maximum power to the patch. The length of this line is optimized for better results and optimized length is equal to13.79 mm.

The concept of spur-line [12] is implemented as shown in fig. 3(a) as band-stop filter with 50 Ω transmission line to switch the operation of the MPA between the frequency bands 3-4 GHz and 5-6 GHz. The length of spur-line is calculated by using equation (1).

$$L_F = \frac{c}{4\, f_{BR}\sqrt{e_{eff}}} \tag{1}$$

where f_{BR} is center frequency of frequency bands that have to be notched and e_{eff} is effective dielectric constant of the material which has been used. Two spur-line BS filters are used. The width of the both spur-line is 0.5 mm. One of them is designed for frequency band centered about 3.5 GHz and other is for frequency band centered about 5.5 GHz.

The inverted T-shaped strip [12] is made on the radiating patch to notch frequency band centered at 4.5 GHz. The length of the strip can be calculated using design equation (2):

$$L_T = \frac{c}{4\, f_{TF}\sqrt{e_{eff}}} \tag{2}$$

where f_{TF} is center frequency of frequency bands that have to be notched.

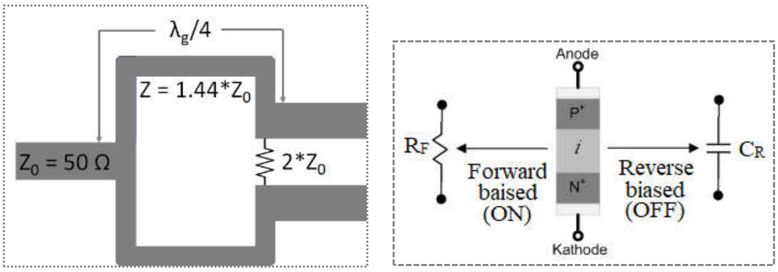

(a) (b)

Figure 1. (a) Wilkinson's power divider (b) PIN Diode and it's equivalent circuits model for ON and OFF state

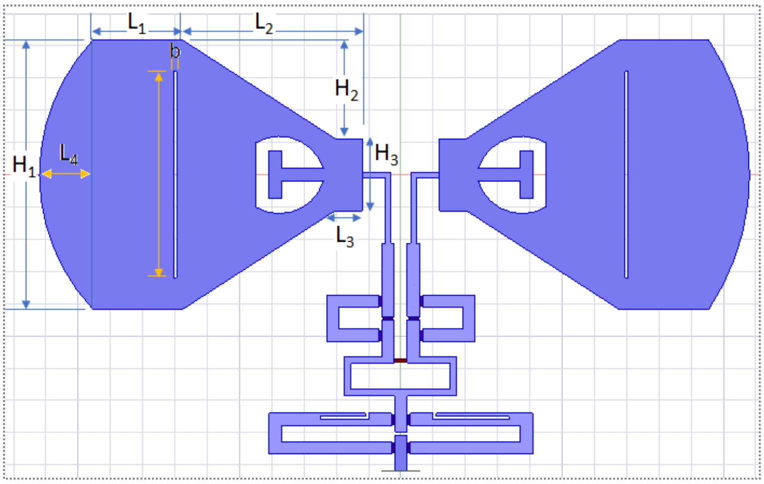

Figure 2. Top view of the designed MPA

The functioning of feed system is controlled by switching states of the PIN diode switches. The operation of filter section of feed system is managed by turning ON the switches S1-S5. When switch S1 turns ON and others are at OFF state, all frequencies at input port are forwarded to the power divider. By turning ON switches S2 & S3and keeping others at OFF state, signal passes through the left side filter of the feed network and the designed antenna doesn't respond for frequency band centered about 5.5 GHz because spur-line based notch filter placed at left side of the feed network is designed at frequency 5.5 GHz. By turning ON switches S4& S5 and keeping others in the OFF state, signal passes through the right side filter and the designed antenna doesn't respond for frequency band centered at 3.5 GHz because spur-line based notch filter placed at right side of feed network is designed at frequency 3.5 GHz. The other controlling part of the feed system is 900 phase shifters. If switches S6 & S9 are turned ON and switches S7, S8, S10 & S11are in OFF state, both signals will reach at the input of radiating patches with same phase as they cover equal lengths of path. If the switches S7, S8 & S9 are turned ON and the switches S6, S10 & S11 are in OFF state, signals at fed to the radiating patches will have 900 phase difference. The antenna behavior for cases will be different and will tune at different resonant frequencies.

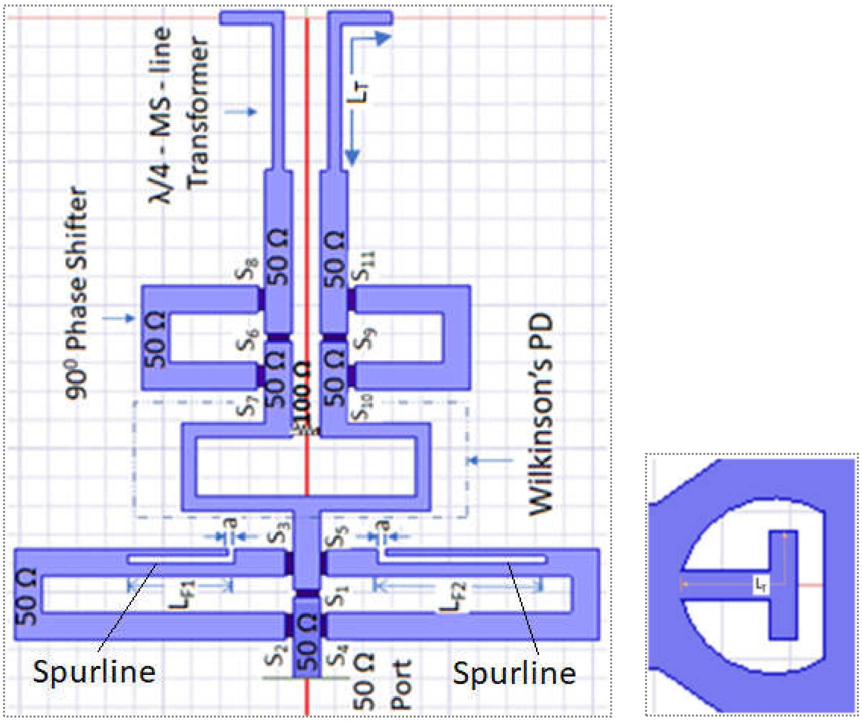

(a) (b)

Figure 3. (a) Design of feed system (b) T-shaped strip line filter

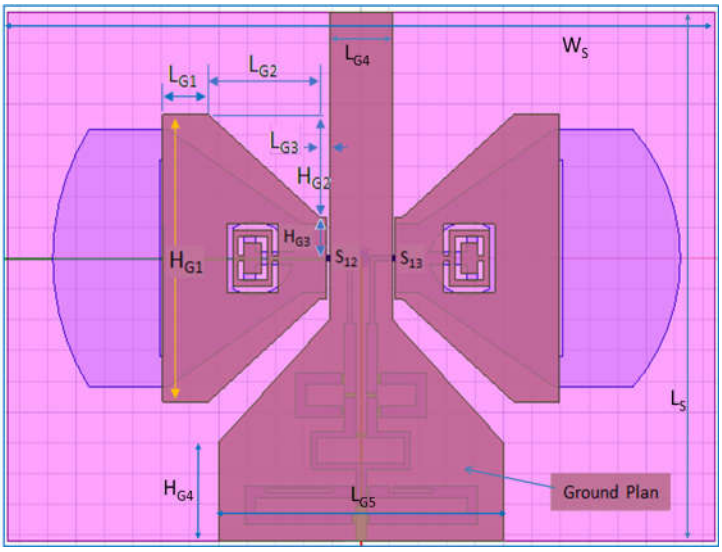

(a)

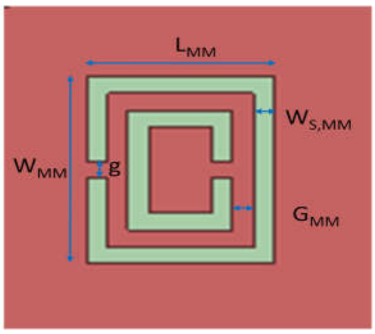

(b)

Figure 4. (a) Bottom layer of the design (b) MM Unit cell

Table 1. Physical Dimension of the designed MPA

Physical Dimensions of the design					
Paramete	**Value (mm)**	**Parameter**	**Value (mm)**	**Parameter**	**Value (mm)**
L_1	14	L_{F2}	11.74	H_{G4}	16
L_2	27.75	L_T	10.24	W_S	124
L_3	4.2	L_{G1}	8	L_S	88
L_4	8.25	L_{G2}	19.55	W_{MM}	11
H_1	41.68	L_{G3}	1.2	L_{MM}	9
H_2	15.24	L_{G4}	11	$W_{S, MM}$	1
H_3	11.2	L_{G5}	50	G_{MM}	1
a	0.5	H_{G1}	46.6	g	1
b	0.5	H_{G2}	16.7		
L_{F1}	7.5	H_{G3}	6.6		

3. Antenna Analysis - Result and Discussion

3.1. Return Loss of designed MPA

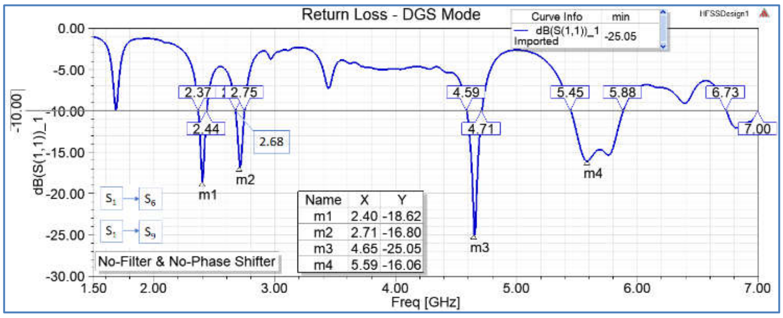

(a)

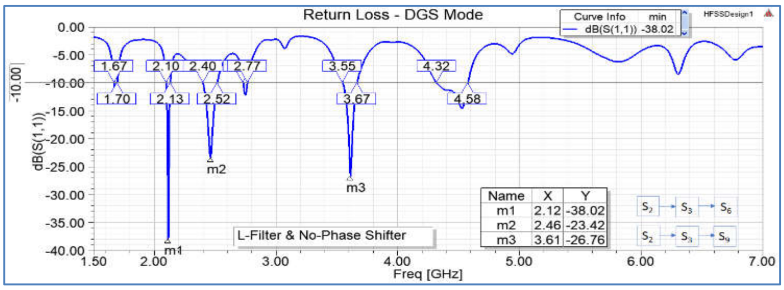

(b)

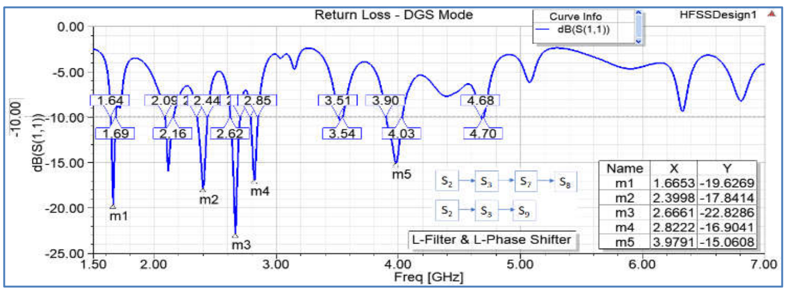

(c)

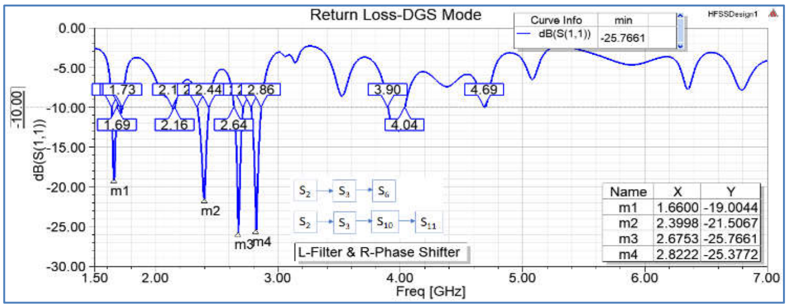

(d)

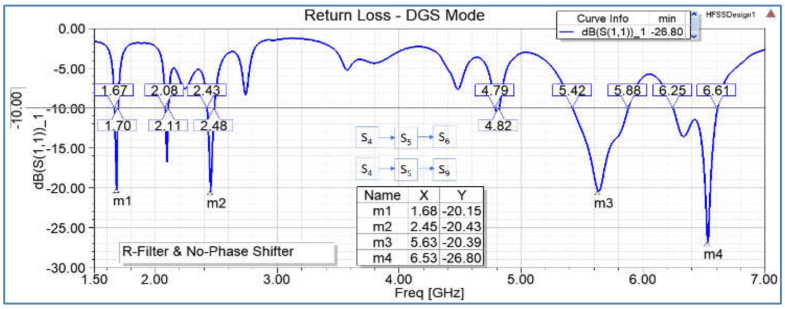

(e)

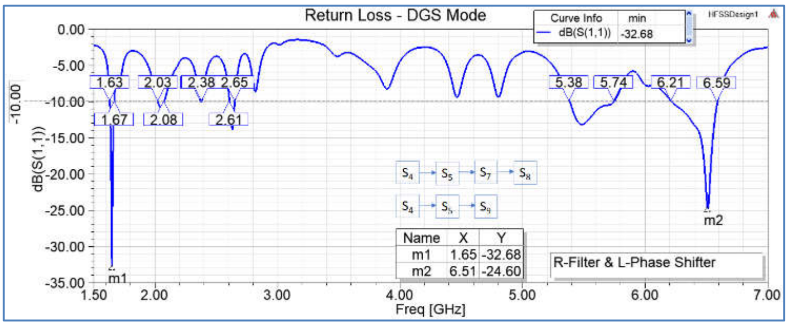

(f)

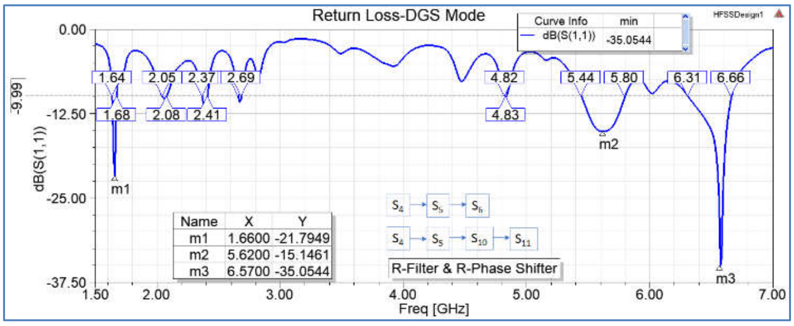

(g)

Figure 5. Return losses of the designed MPA for DGS Mode (a) No filter & No phase shifter (b) L-filter & No-PS (c) L-filter & L-PS (d) L-filter & R-PS (e) R-filter & No-PS (f) R-filter & L-PS (g) R-filter & R-PS

The reflection coefficient, S11 of the designed antenna for DGS mode is depicted in fig. 5 for various combinations of switches in active position. It is clearly observed that when the right-sided filter is activated then lower frequencies (3-4 GHz) is filtered out since right-sided filter is designed for filtering lower frequencies and when the left-sided filter is activated then higher frequencies (5-6 GHz) is filtered out since left-sided filter is designed for filtering higher frequencies. It is also noticed that phase shifter has no much more impact on configuring the operational frequency of the designed MPA. From figure fig. 5(a), the designed MPA resonates at frequencies 2.40, 2.71, 4.65 & 5.59 GHz with maximum impedance BW of 70, 70, 120 & 430 GHz respectively. From fig. 5(b), the designed MPA tunes at frequencies 2.12, 2.46 & 3.61 GHz with maximum IBW of 30, 120 & 120 GHz respectively. From fig. 5(e), the designed MPA tunes at frequencies 1.68, 2.45, 5.63 & 6.53 GHz. Thus from fig. 5(a, b & e), the designed MPA's operation can be switched among various groups of frequencies. From fig. 5(b, c & d), the designed antenna's response can be configured between 3.61GHz and 3.97 GHz.

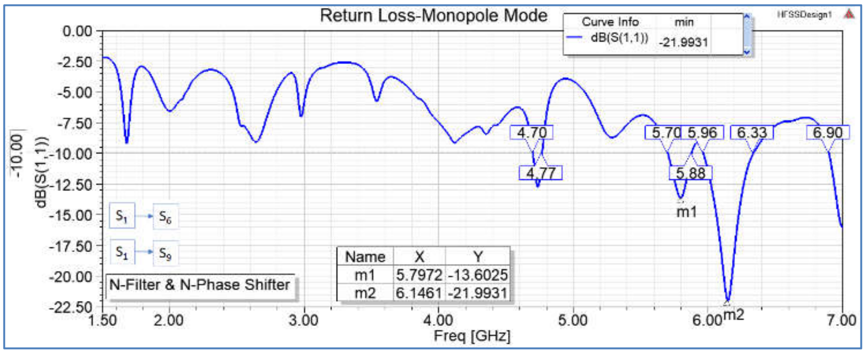

(a)

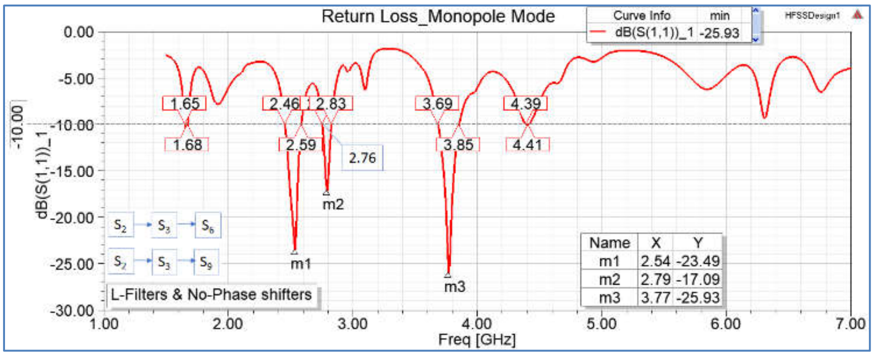

(b)

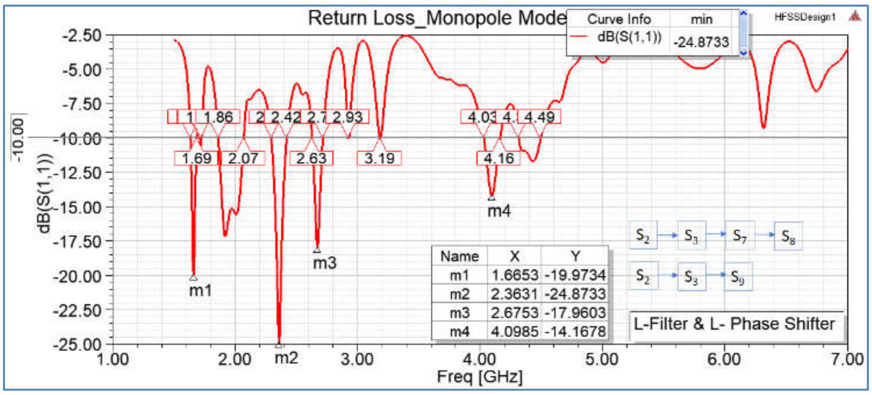

(c)

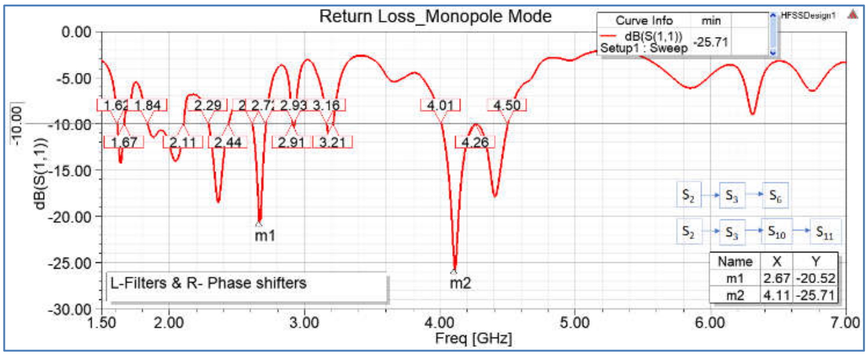

(d)

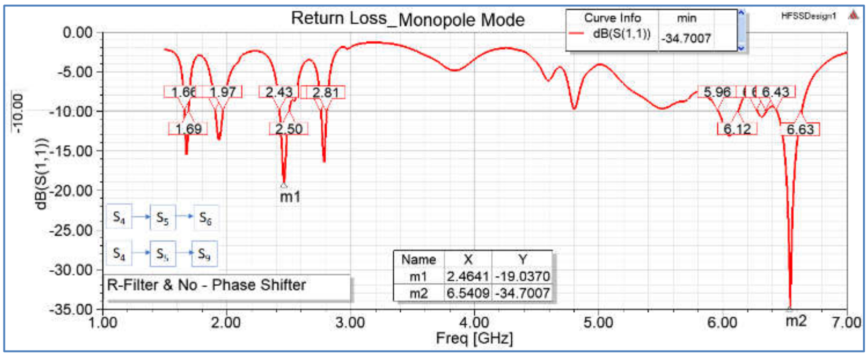

(e)

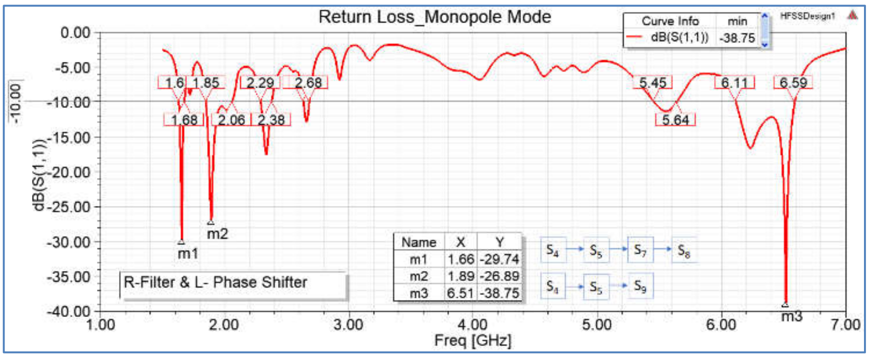

(f)

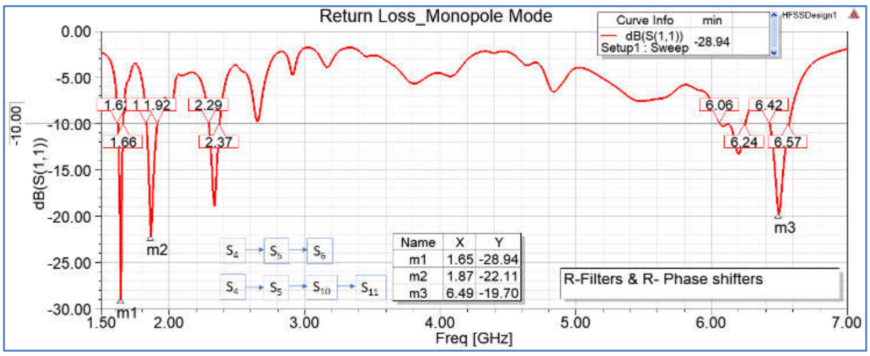

(g)

Figure 6. Return losses of the designed MPA for monopole Mode (a) No filter & No phase shifter (b) L-filter & No-PS (c) L-filter & L-PS (d) L-filter & R-PS (e) R-filter & No-PS (f) R-filter & L-PS (g) R-filter & R-PS

The reflection coefficient, S11 of the designed antenna for monopole mode is plotted in fig. 6 for various combinations of switches in active position. From fig. 6(a), the designed

MPA resonates at 6.14 GHz (IBW = 370 GHz). The designed antenna responds only at frequencies 2.54 GHz and 3.77 GHz with IBW of 130 GHz & 160 GHz as shown in the fig. 6(b) since left-sided filter is activated which suppressed frequencies between 5-6 GHz. The designed antenna responds at frequencies 2.46 GHz & 6.56 GHz as shown in fig. 6(e), when right-sided filter is activated which filters out frequencies between 3-4 GHz. In fig. 6(c & d), frequencies between 5-6 GHz are filtered out as left-sided filter is activated where as in fig. 6(f & g), frequencies between 3-4 GHz are filtered out as right-sided filter is activated. Thus designed MPA's response can be switched between frequency spans 3-4 GHz and 5-6 GHz by activating ether right-sided filter on left-sided filter.

3.2. Gain of designed MPA

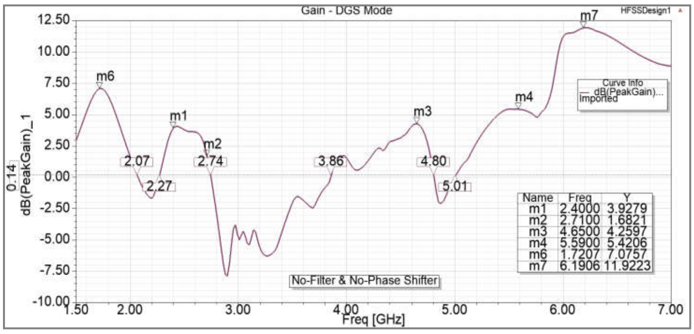

(a)

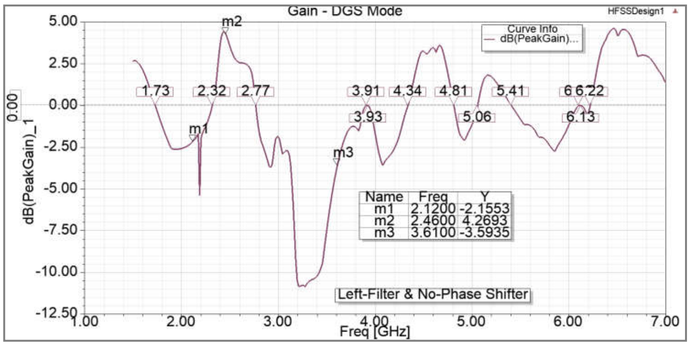

(b)

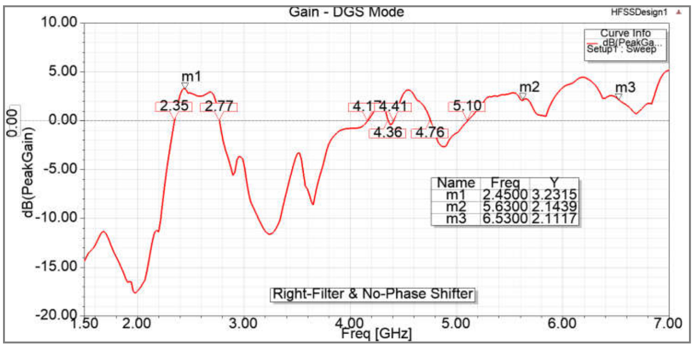

(c)

Figure 7. Peak Gain v/s frequency plot of the designed MPA for DGS Mode (a) No-filter & No-phase shifter (b) L-filter & No-PS (b) R-filter & No-PS

The gain of the designed MPA for the DGS Mode is plotted for the frequencies ranging from 1.5 GHz to 7 GHz in fig. 7. Fig. 7(a) is showing the peak gain verse frequency plot when neither of filter is activated and the maximum gain of 3.92 dB, 1.68 dB, 4.25 dB & 5.40 dB is obtained at frequencies 2.40, 2.71, 4.65 & 5.59 GHz. Fig. 7(b & c) is showing the peak gain verse frequency plot when either left-sided filter is activated or right-sided filter is activated respectively. The peak gain of -2.15 dB, 4.26 dB & -3.59 dB at frequencies 2.12, 2.46 & 3.61 GHz when left-sided filter is activated. The peak gain of 3.23 dB, 2.14 dB & 2.11 dB at frequencies 2.45, 5.63 & 6.53 GHz is attained when right-sided filter is activated. It is observed from the fig. 7(a & c) that positive gain is obtained for the frequencies for which return losses are below -10dB.

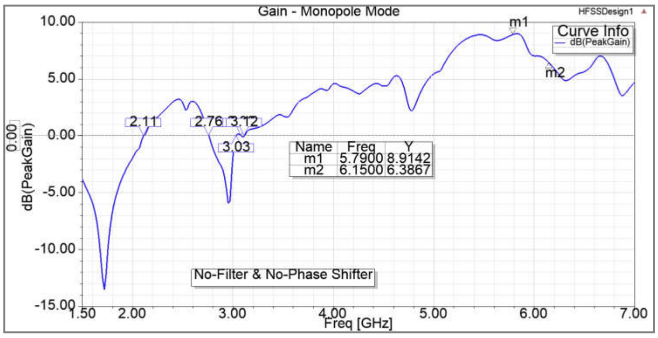

(a)

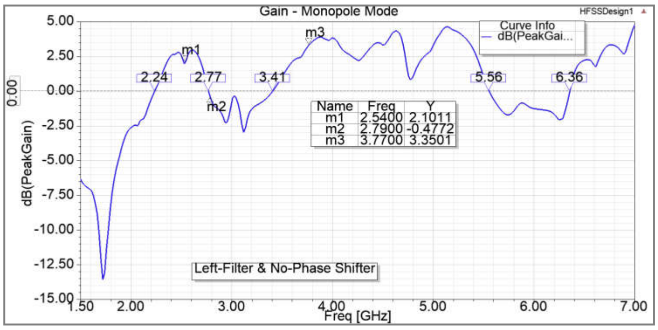

(b)

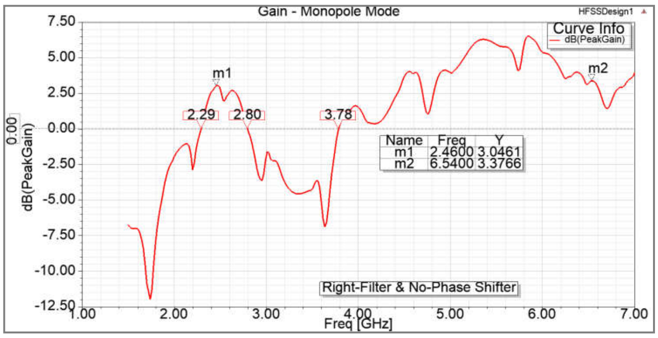

(c)

Figure 8. Peak Gain v/s frequency plot of the designed MPA for monopole Mode (a) No-filter & No-phase shifter (b) L-filter & No-PS (b) R-filter & No-PS

The gain of the designed MPA for the monopole mode is plotted for the frequencies ranging from 1.5 GHz to 7 GHz in fig. 8. The peak gain verse frequency is plotted in fig. 8(a) for neither of filters is activated and the peak gain of 8.9 dB & 6.38 dB is obtained at resonating frequencies 5.79 GHz & 6.15 GHz respectively. Fig. 8(b) is demonstrating the peak gain for active state of the left-sided filter and peak gain of 2.10 dB, -0.47 dB & 3.35 dB is attained at resonating frequencies 2.54 GHz, 2.79 GHz & 3.77 GHz respectively. The peak gain of the designed MPA is given in fig. 8(c) when right-sided filter is activated and peak gain of [3.04 & 3.37] dB, is obtained at resonating frequencies 2.46 GHz & 6.54 GHz.

3.3. Radiation Pattern of designed MPA

The 3-D graphical scenario of the radiation radiated by the designed MPA is pictured in figures 9 & 10. Each figure shows two different patterns: E-plane & H-plane pattern. The fig. 9 is demonstrating the radiation patterns when designed MPA was functioning in DGS mode where as the radiation patterns displayed in fig. 10 are 3-D graphical representation of radiated energy when designed MPA was functioning in monopole (MP) mode. It has been inspected that each patterns exhibits a multi-directive nature in both planes. Fig. 9(a) exhibits the radiation patterns for frequencies 2.40, 2.71, 4.65 & 5.59 GHz for DGS mode when neither of filter nor phase shifter is activated. The radiation patterns for frequencies 2.46 & 3.71 GHz for DGS mode is displayed in fig. 9(b) when only the left-sided filter is activated. Fig. 9(c) exhibits the radiation patterns for frequencies 2.45 & 5.63 GHz for DGS mode when only the right-sided filter is activated.

Fig. 10(a) exhibits the radiation patterns for frequencies 5.78 & 6.15 GHz for MP mode when neither of filter nor phase shifter is activated. Fig. 10(b) exhibits the radiation patterns for frequencies 2.54 & 3.77 GHz for MP mode when only the left-sided filter is activated. Fig. 10(c) exhibits the radiation patterns for frequencies 2.46 & 6.54 GHz for MP mode when only the left-sided filter is activated.

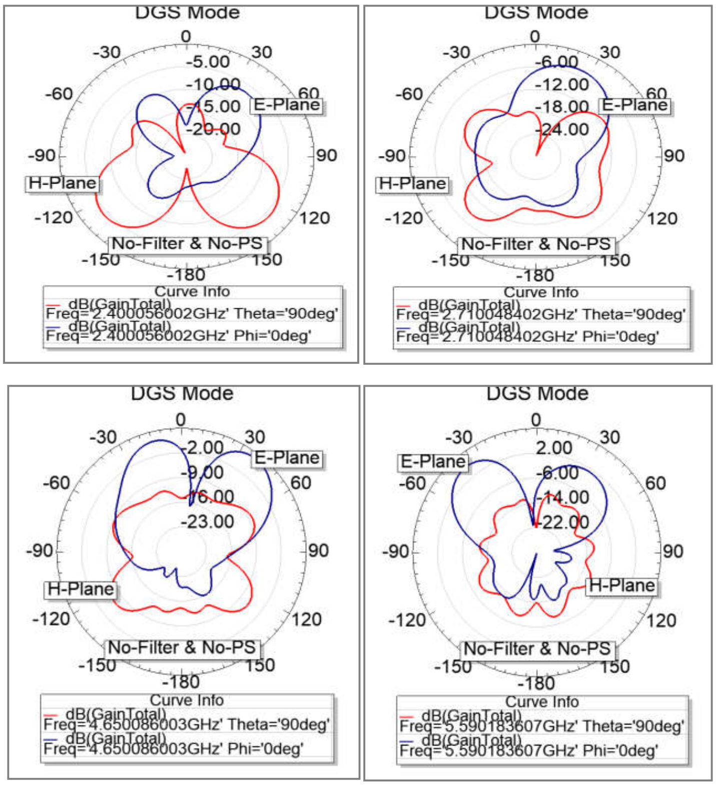

(a)

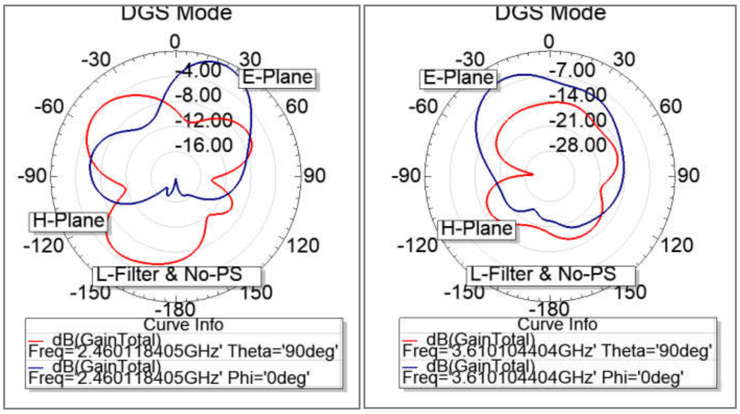

(b)

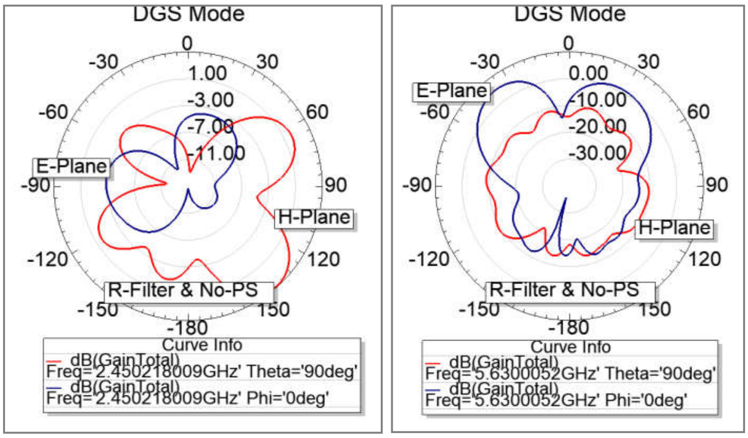

(c)

Figure 9. Radiation Pattern of the designed MPA for DGS Mode (a) No-filter & No-phase shifter (b) L-filter & No-PS (b) R-filter & No-PS

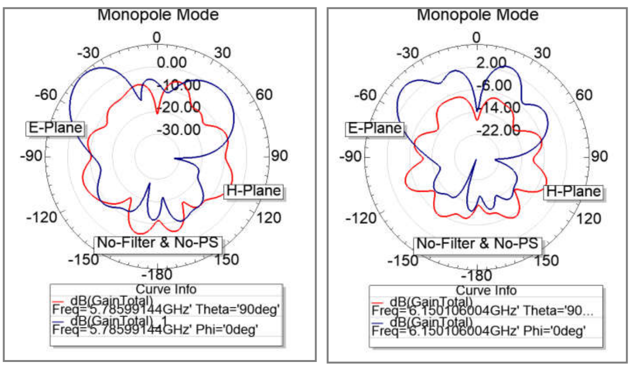

(a)

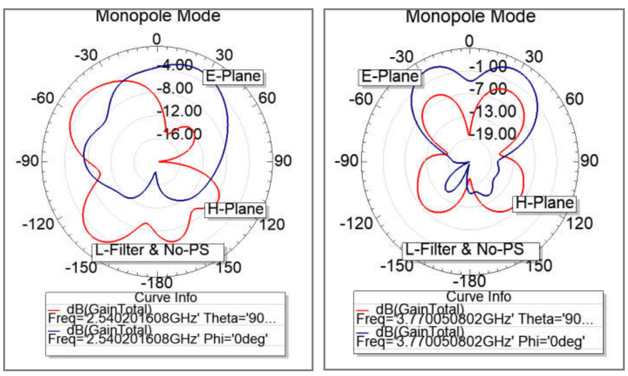

(b)

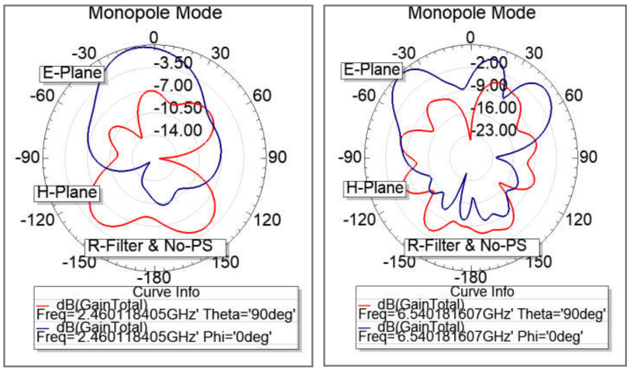

(c)

Figure 10. Radiation Pattern of the designed MPA for monopole Mode (a) No-filter & No-phase shifter (b) L-filter & No-PS (b) R-filter & No-PS

3.3. Axial Ratio of designed MPA

Axial Ratio of the designed MPA for DGS mode and monopole mode is depicted in fig. 11. Fig 11(a & b) shows the axial ratio of the designed MPA when designed MPA was functioning in DGS mode. In fig. 11(a), three different plots are shown for various activating status of filters when right-sided PS is activated. When right-sided PS is activated then RHCP is achieved. It is observed that frequency bands those have AR below 3 dB get changed when either left-sided filter or right-sided filter or none of them is activated. For circular polarization, the practical acceptable value of AR is below 3 dB. Thus frequency bands (AR < 3dB) can be switched to others for RHCP mode by changing the active status of the filters. The center frequencies for various AR-3dB frequency bands for RHCP mode are 4.31 GHz (AR_3-dB BW = 0.92%), 5.06 GHz (0.99%), 5.38 GHz (1.49%), 5.54 GHz (2.18%), 5.64 GHz (0.35%), 5.76 GHz (1.56%), 5.80 GHz (0.52%), 6.34 GHz (0.16%). In fig. 11(b), various plots are sketched when left-sided PS is activated. Thus LHCP mode will dominate. The frequencies, at which maximum AR for LHCP mode is obtained, are 4.46 GHz (0.90%), 4.54 GHz (1.32%), 5.26 GHz (4.75%), 5.84 GHz (0.51%) & 6.04 GHz (1.33%).

The axial ratio of the designed MPA is depicting in fig 11(c & d) when designed MPA was functioning in monopole mode. In fig. 11(c), three different plots are sketched when right-sided PS is activated. Thus RHCP mode will dominate. The frequencies, at which maximum AR for RHCP mode is obtained, are 4.98 (AR_3-dB BW = 1%), 5.04 (1%), 5.10 (2.55%), 5.24 (1.90%), 6.56 (0.76%), 6.94 (0.58%), 5.12 (0.4%), 6.72 (0.3%). In fig. 11(d), three different plots are sketched when left-sided PS is activated. The frequencies, at which maximum AR for LHCP mode is obtained, are 1.64 (1.22%), 1.88 (1.6%), 5.28 (1.14%), 6.52 (2.30%), and 6.54 (0.31%).

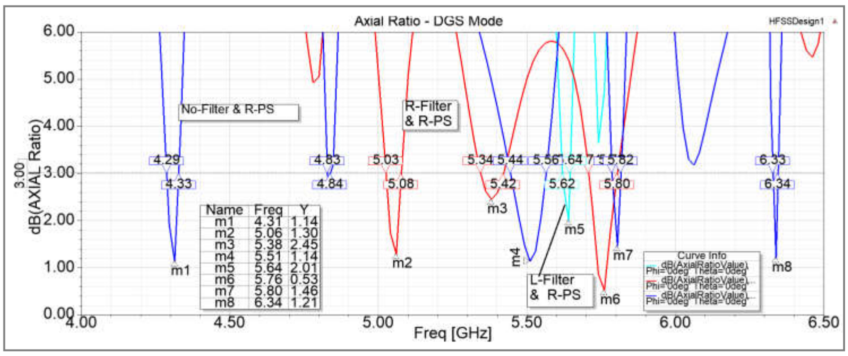

(a)

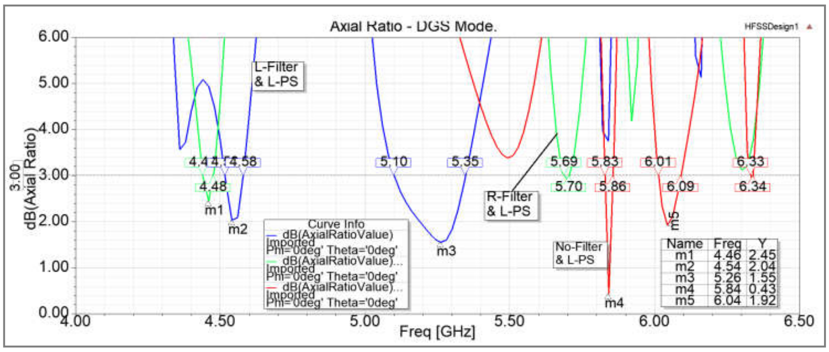

(b)

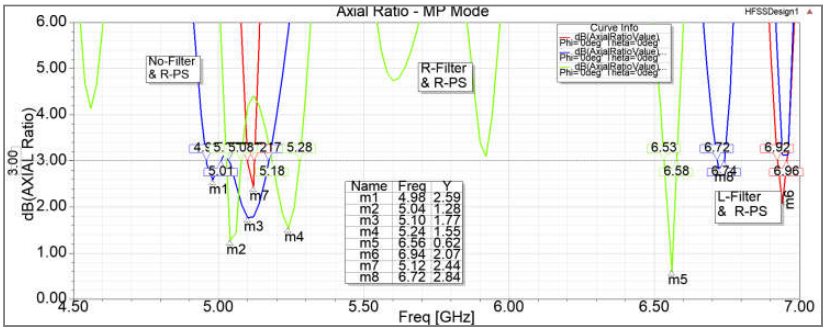

(c)

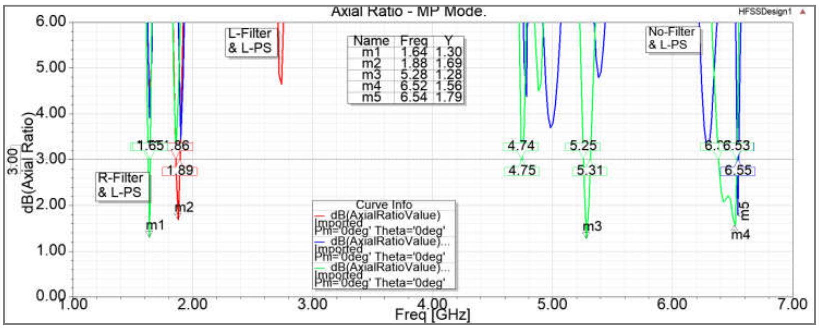

(d)

Figure 11. Axial Ratio of the designed MPA (a) DGS Mode – Right-sided phase shifter activated (b) DGS Mode – Left-sided phase shifter activated (c) Monopole Mode – Right-sided phase shifter activated (d) Monopole Mode – Left-sided phase shifter activated

4.Conclusion

The designed MPA which consists of a bow-tie shaped patch, switchable ground plane and feed network is presented. The filtering technique is utilized with feed network to filter out two groups of frequencies 3-4 GHz and 5-6 GHz. The designed MPA can operate in either DGS mode or monopole mode. In this way, the operational frequency of the designed MPA can be reconfigured among various frequency bands. The designed MPA also incorporates to reconfigure mode of polarization (LHCP & RHCP). The switching mechanism is utilized to switch the operation of the antenna in various frequency bands. The designed MPA in DGS mode is incorporate to tune at frequencies [2.12, 2.46 & 3.61] GHz with maximum IBW of 30, 120 & 120 GHz and maximum gain of -2.15 dB, 4.26 dB & -3.59 dB respectively when the left-sided filter of the feed network is activated where as it can operate at frequencies [1.68, 2.45, 5.63 & 6.53] GHz when the right-sided filter is activated. The peak gain of 3.23 dB, 2.14 dB & 2.11 dB is gained at frequencies 2.45, 5.63 & 6.53 GHz when right-sided filter is activated in DGS mode. The designed antenna in monopole mode responds only at frequencies 2.54 GHz and 3.77 GHz with IBW of 130 GHz & 160 GHz and peak gain of 2.10 dB & 3.35 dB since left-sided filter is activated which suppressed frequencies between 5-6 GHz. whereas the designed antenna responds at frequencies 2.46 GHz & 6.56 GHz with peak gain of 3.04 dB & 3.37 dB when right-sided filter is activated which filters out frequencies between 3-4 GHz. The antenna structure is incorporated to work in S-band, C-band. The S-band applications involve areas such as RFID, weather radar, surface ship radar etc.. The C-band is incorporated to satellite communications like satellite TV networks because of less susceptible to rain fade than Ku-band.

REFERENCES

[1] *Sung-Woong Choi, Young-Bae Jung and Seong-Ook Park, "Multi-band and multi-polarized reconfigurable antenna for next generation mobile communication base-station applications," IET Microwaves, Antennas & Prop., Vol. 7, No. 10, pp. 819 – 824, 2013*

[2] *Yunfei Cao, S. W. Cheung and T. I. Yuk; "A Simple Planar Polarization Reconfigurable Monopole Antenna for GNSS/PCS," IEEE TRANSACTIONS ON ANTENNAS AND PROPAGATION, VOL. 63, NO. 2, pp. 500-507, FEBRUARY 2015*

[3] *Tong Li, Huiqing Zhai, Long Li and Changhong Liang, "Frequency-Reconfigurable Bow-Tie Antenna With a Wide Tuning Range," IEEE Antennas and Wireless Prop. Letters, Vol. 13, pp. 1549-52, 2014*

[4] *Peng Kai Li, Zhen Hai Shao, Quan Wang, and Yu Jian Cheng, 'Frequency- and Pattern-Reconfigurable Antenna for Multistandard Wireless Applications', IEEE ANTENNAS AND WIRELESS PROPAGATION LETTERS, VOL. 14, pp. 333-336, 2017*

[5] *S. Raman, P. Mohanan and Nick Timmons, "Microstrip-Fed Pattern- and Polarization-Reconfigurable Compact Truncated Monopole Antenna," IEEE ANTENNAS AND WIRELESS PROPAGATION LETTERS, VOL. 12, pp. 710-713, 2013*

[6] *Eduardo Jorge Brito Rodrigues and Hertz Wilton Castro Lins "Fast and accurate synthesis of electronically reconfigurable annular ring monopole antennas using particle swarm optimization and artificial bee colony algorithms," IET Microwaves, Antennas & Propagation, pp. 362-369, 2016*

[7] *Devesh Kumar and Anwar S. Siddiqui, "Design, Simulation and a Comparative study of Square, Rectangular, Triangular and Dual Beamed RF MEMS Switch for Switching Applications," IEEE conference SPIN 2017, pp. 270-274, Feb 2017.*

[8] *ZHANG Pengfei, LIU Shizhong and CHEN Rongrong, 'A Reconfigurable Microstrip Patch Antenna with Frequency and Circular Polarization Diversities', Chinese Journal of Electronics Vol.25, No.2, pp. 381-383, Mar. 2016*

[9] *Devesh Kumar, Anwar Shahzad Siddiqui, H. P. Singh, 'A Review: Techniques and Methodologies Adopted for Reconfigurable Antennas ', IEEE Conference SEEMS 2018, Oct. 2018.*

[10] *Nghia Nguyen-Trong and Christophe Fumeaux, 'A Frequency- and Pattern-Reconfigurable Center-Shorted Microstrip Antenna', IEEE ANTENNAS AND WIRELESS PROPAGATION LETTERS, VOL. 15, pp. 1955-1958, 2016*

[11] *Devesh Kumar, Anwar Shahzad Siddiqui, H. P. Singh, 'Monopole Concept Based Frequency Reconfigurable Patch Antenna for mm-Wave 5G-Band Applications', IEEE Conference SPIN 2019, pp. 141-145, March 2019.*

[12] *M. Moosazadeh, A.M. Abbosh and Z. Esmati; "Design of compact planar ultra-wideband antenna with dual-notched bands using slotted square patch and pi-shaped conductor-backed plane" IET Microw. Antennas Propagation, Vol. 6, Issue 3, pp. 290–294, 012*

[13] *PIETER J. VAN VLIET & JOSEPH L. TAURITZ "Practical design of microstrip spur-line bandstop filters", International Journal of Electronics, vol 69, No. 5, pp. 697-703, 1990*

[14] *Abhijeet Kumar, Prity Mishra and Savita Kadian; "An Overview on Microstrip Spurline Bandstop Filter" International Journal of Emerging Technologies and Engineering (IJETE), Volume 1 Issue 6, pp. 165-170, July 2014.*

[15] *Hubregt J. VISSER, "Array and Phased Array Antenna Basics", John Wiley & Sons, Ltd, 2005*